Polymer 272 (2023) 125861

Contents lists available at ScienceDirect

Polymer

journal homepage: www.elsevier.com/locate/polymer

Incorporating GSE4 peptide in PEG/hyaluronic acid hydrogels to promote the alveolar epithelial differentiation of mesenchymal stem cells

Xiaoqiong Wang [a,b], Leisha Cui [c], Jing Hong [c], Zhaojun Wang [c], Jiawei Li [c], Zhongqing Liu [c], Zhanchi Zhu [c], Ying Hao [c,*], Guosheng Cheng [c,**], Junhong Jiang [a,d,***]

[a] Department of Pulmonary and Critical Care Medicine, The First Affiliated Hospital of Soochow University, Suzhou, 215006, Jiangsu Province, China
[b] Department of Pulmonary and Critical Care Medicine, The Second People's Hospital of Hefei, Hefei Hospital Affiliated to Anhui Medical University, Hefei, 230011, Anhui Province, China
[c] CAS key Laboratory of Nano-Bio Interface, Suzhou Institute of Nano-Tech and Nano-Bionics, Chinese Academy of Sciences, Suzhou, 215123, Jiangsu Province, China
[d] Department of Pulmonary and Critical Care Medicine, Dushu Lake Hospital, Affiliated to Soochow University, Suzhou, 215000, Jiangsu Province, China

ARTICLE INFO

Keywords:
Hydrogel
Mesenchymal stem cells
Differentiation
Type II alveolar Epithelial cells
Peptide

ABSTRACT

Because of the shortage of donors, alveolar stem cells transplantation is under development as an important and promising treatment for end-stage lung disease. Currently, the acquisition of functional lung cells is mostly performed by two dimensional (2D) culture and suffers from low directed differentiation efficiency. It is particularly critical to replicate the three dimensional (3D) growth of lung cells, as cells grow in 3D microenvironment *in vivo*. In this work, we develop a 3D biomimetic composite hydrogel system based on the *in situ* crosslinking of the synthetic polymer 4 arm acrylated-poly(ethylene glycol) (4PEG-AC), the thiolated natural polymer hyaluronic acid (HA-SH), and the thiolated polypeptide (GSE4-SH) via a Michael-type "click" reaction under physiological conditions at pH 7.8. The PEG/HA/GSE4 hydrogel with a sheer modulus of 104.1 ± 9.9 Pa was used for 3D growth of bone marrow mesenchymal stem cells (BMSCs), displaying excellent biocompatibility. Covalent conjugation of GSE4 peptide in hydrogel promoted the differentiation of BMSCs into alveolar epithelial type 2 cells (AEC2s) with a AEC2s-differentiation rate of 58.6 ± 3.3%. Overall, this study provides a suitable 3D biomimetic platform to enable the efficient differentiation of stem cells into lung cells for lung tissue engineering.

1. Introduction

The respiratory system plays a vital role in human life. It is subjected to a variety of environmental toxins, including allergens, pollution, irritants, smoke, and viral or bacterial infections, all of which can continuously damage or kill alveolar epithelial cells. In turn, the lungs actively repair damaged cells by causing alveolar stem cells to multiply and change into different types of cells [1]. Many diseases of the respiratory system, such as pulmonary fibrosis, acute lung injury, and emphysema, lack curative drugs. Currently, lung transplantation remains the only treatment for end-stage conditions, but challenges still exist in view of the shortages of donors, complicated procedure, low success rates, high mortality rates, and enormous costs of lung transplantation. A large number of researches support the efficacy of pulmonary seed cells in the treatment of pulmonary disease, which has been emerged as a promising therapeutic approach [2–4].

The human alveoli are composed of type I alveolar epithelial cells (AEC1s) and type II alveolar epithelial cells (AEC2s). AEC2s make up 15% of the lung parenchyma cells, showing a distinctive cuboidal shape. Numerous animal studies have shown that AEC2s can renew AEC1s during the steady state or after injury [5]. Pulmonary surfactant proteins, including surfactant protein A, B, C and D (SPA, SPB, SPC, and SPD), are mainly synthesized by AEC2s. Among them, SPC can be synthesized only by AEC2s and thus is considered an AEC2 marker [5]. Therefore, it is important to obtain sufficient AEC2s for stem cell therapy in lung tissue engineering. Various stem cell types have been chosen to enhance the potential differentiation of stem cells into AEC2s, such as mouse bone marrow mesenchymal stem cells (mBMSCs), mouse adipose

* Corresponding author.
** Corresponding author.
*** Corresponding author. Department of Pulmonary and Critical Care Medicine, The First Affiliated Hospital of Soochow University, Suzhou, 215006, Jiangsu Province, China.
E-mail addresses: yhao2017@sinano.ac.cn (Y. Hao), gscheng2006@sinano.ac.cn (G. Cheng), jiangjunhong1969@suda.edu.cn (J. Jiang).

https://doi.org/10.1016/j.polymer.2023.125861
Received 23 December 2022; Received in revised form 5 March 2023; Accepted 8 March 2023
Available online 9 March 2023
0032-3861/© 2023 Elsevier Ltd. All rights reserved.

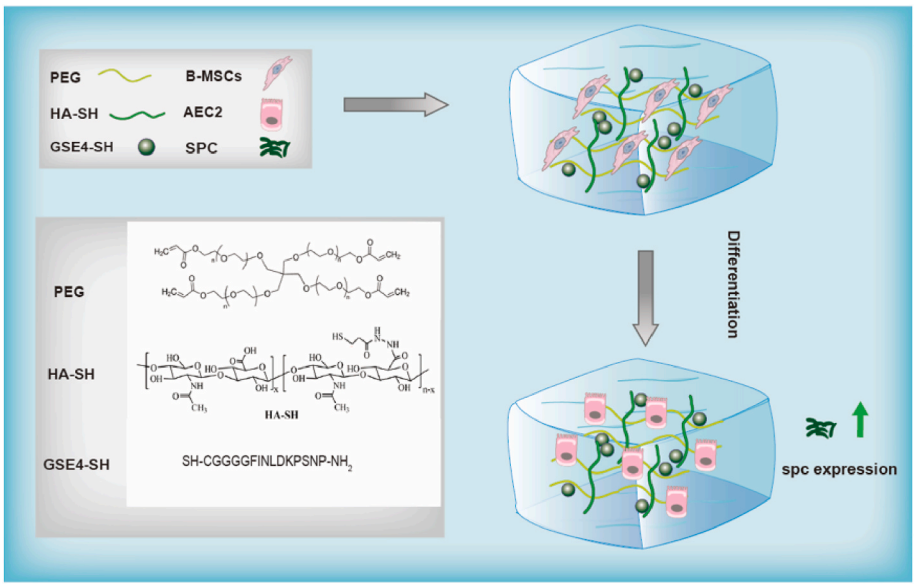

Fig. 1. Schematic illustration of PEG/HA/GSE4 hydrogel fabrication for AEC2-differentiation of BMSCs.

tissue-derived stem cells, and human umbilical cord mesenchymal stem cells (hUMSCs) [6–11]. The differentiated AEC2s successfully repaired lung damage caused by pulmonary fibrosis [10] or emphysema [11]. Mesenchymal bone marrow stem cells (BMSCs) are a type of pluripotent stem cell that is easy to extract from tissues. The advantages of multi-directional differentiation potential, low immunogenicity, and a low tumorigenic risk with no ethical controversy make them ideal for tissue engineering. Although many approaches have been used to increase differentiation efficiency, the problem of low differentiation efficiency remains. Besides, in traditional two-dimensional (2D) culture, the physiological interactions among or between cells and the matrix cannot be realistically reproduced. Alternatively, three-dimensional (3D) culture can better replicate the *in vivo* microenvironment of stem cells [12,13]. With the development of materials science, cell culture in a 3D environment has been achieved by using 3D scaffold biomaterials [14,15]. Owing to the unique physical and chemical properties, hydrogels have become ideal biomaterials to mimic the extracellular matrix (ECM) [16,17]. *In vitro*, the differentiation of stem cells into osteogenic cells, chondrogenic cells, neurons and cardiomyocytes has been achieved in a 3D hydrogel network with high differentiation efficiency and repair effects for corresponding damaged tissues [18]. Nevertheless, the differentiation of stem cells into alveolar epithelial cells in a 3D hydrogel network has been less reported. In addition, it has been proved that the conjugation of biological factors such as peptides in hydrogel matrix efficiently facilitated the differentiation of stem cells [15].

Herein, we designed and fabricated a composite hydrogel based on poly(ethylene glycol) (PEG), hyaluronic acid (HA), and GSE4 peptide. Specifically, the natural polymer HA, as a ECM component, was chemically modified by reacting the carboxyl group to a thiol (-SH) group to yield HA-SH. Subsequently, HA-SH was cross-linked with a 4 arm acrylated and Drug Administration (FDA) approved synthetic polymer PEG (4PEG-AC) to form hydrogels *in situ*. GSE4 peptide was designed to install thiol group as GSE4-SH by adding glycine and cysteine, endowing peptide with water solubility and acrylate reactivity, respectively. The mechanical properties and morphologies of PEG/HA/GSE4 hydrogels were examined. Then, the hydrogel was used for 3D culture of BMSCs (Fig. 1). The cell viability and the effect of incorporated GSE4 on the AEC2s-differentiation of BMSCs were investigated by live/dead assay, immunofluorescence staining and real-time quantitative polymerase chain reaction (RT-qPCR).

2. Experimental section

2.1. Materials

HA (sodium salt, Mw 403.31 KDa, 95%, Macklin), DL-dithiothreitol (DTT,99%,Aladdin), N-(3-dimethylaminopropyl)-N′-ethylcarbodiimide hydrochloride (EDCI, 98%, Sigma-Aldrich), 3,3′-dithiobis(propanoic dihydrazide) (DTP, 98%, J&K Scientific), foetal bovine serum (FBS, Gibco, Australia), Dulbecco's modified Eagle medium with F-12 nutrient mixture (DMEM/F-12 Gibco, Australia), Penicillin-Streptomycin Solution (Procell, China), Trypsin-EDTA (0.25%: 0.02%) (Sigma-Aldrich), BMSCs and human small airway epithelial cells in complete medium (SAEpiCM) were purchased from Procell Life Science & Technology Co, Ltd. Immunol Staining Fix Solution, Immunol Staining Wash Buffer, Immunostaining Permeabilization Solution with Saponin, Immunol Staining Blocking Buffer and DAPI dihydrochloride were obtained from Beyotime Inc. The Calcein-AM/PI Cell Viability/Cytotoxicity Assay Kit was purchased from Biosharp Biotechnology. Anti-Prosurfactant Protein C antibody, Anti-Prosurfactant Protein B antibody, goat anti-rabbit IgG H&L (Alexa Fluor 594) and goat anti-mouse IgG H&L (Alexa Fluor 488) were obtained from Abcam Life Technology. TRIzol was purchased from Thermo Fisher Scientific. 4ARM-PEG-acrylate (PEG) was purchased from JenKem Technology. GSE4-SH (Ac-CGGGGFINLDKPSNP-NH_2, 98.38%) was custom-synthesized by ChinaPeptides Co., Ltd.

2.2. Synthesis and characterization of hydrogel

According to the reported methodology [19], HA-SH was produced by combining DTP with EDCI in an aqueous medium at pH 4.75 and then reducing it with DTT. After being dialyzed to remove unreacted materials, the product was lyophilized. The degree of modification was calculated based on ^{1}H NMR. HA-SH and 4PEG-AC were individually dissolved in PBS at a concentration of 2 wt%. GSE4-SH (2 mM) was added to the mixtures of HA-SH and 4PEG-AC. Gelation was initiated by combining the aforementioned solutions with NaOH and adjusting the solution's pH to 7.8. Hydrogel were frozen using liquid nitrogen and then lyophilized, followed by the sputter-coating with gold at 5k eV and 30 mA for 2 min to then visualize the morphology of PEG/HA/GSE4 hydrogels via scanning electron microscopy (SEM, Quanta 400 FEG, FEI, USA).

To measure the swelling ratio of hydrogels, freshly prepared hydrogel disks were incubated in PBS 7.4 at 37 °C for 24 h. Then,

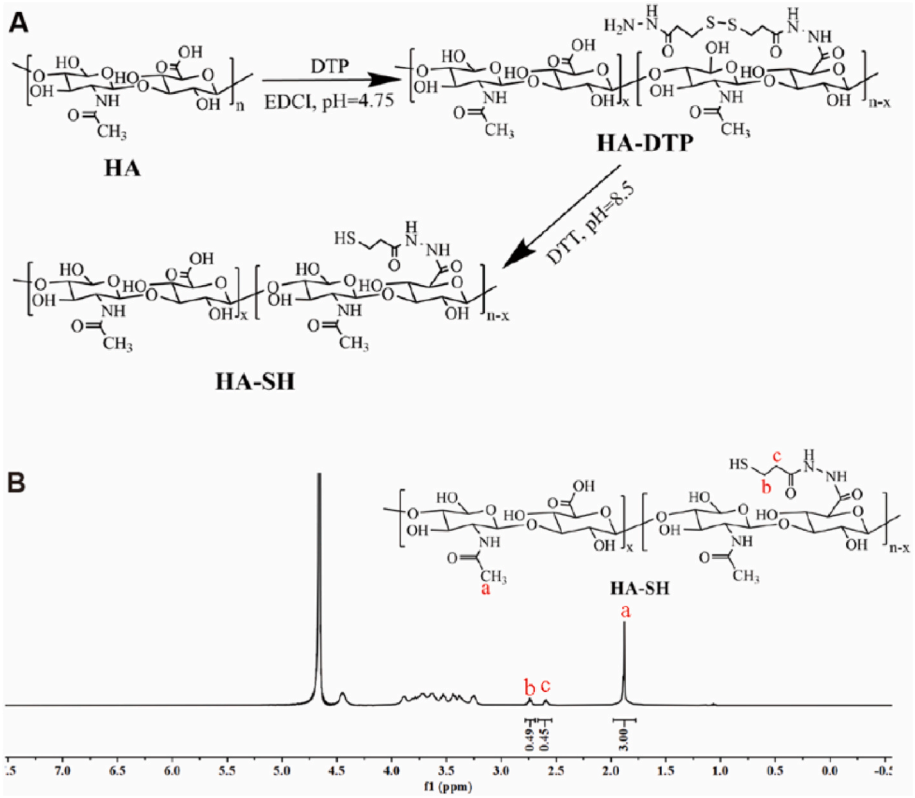

Fig. 2. Synthesis route (A) and ^{1}H NMR spectrum (B) of HA-SH.

individual disks were washed thoroughly with DI water, followed by the dehydration by using graded ethanol solutions and dried at 37 °C overnight. The dry weight (W_d) was recorded. Then, hydrogel samples were re-immersed in PBS for 48 h and the wet weight (W_w) was measured at predetermined time until the swelling equilibrium was reached. The swelling ratio (SW) was calculated as SW = W_w/W_d. Additionally, degradation behavior of the hydrogels was estimated by measuring the residual hydrogel weight. Hydrogel disks were immersed in PBS 7.4 with or without 30 U/mL HAase enzyme. The medium was replenished at a predetermined time, and the mass of hydrogels were recorded as W_t. At each time point, hydrogel content (wt%) in the remaining hydrogels was calculated as $(W_0\text{-}W_t)/W_0$*100, where W_0 is the initial hydrogel mass in each sample. The measurements were performed in triplicate and the results were expressed as the mean ± standard derivation (SD).

The oscillatory rheology was analyzed by a rheometer (RS6000, Thermo Haake) with a 20 mm parallel plate geometry. As mentioned previously, a precursor solution of HA-SH and 4PEG-AC containing GSE4-SH was prepared. Then, 100 μL of precursor solution was placed on the test platform. The DI water was applied in a geometric pattern with a spacing of 200 μm to keep the hydrogel from drying out. Subsequently, the gelation process was initiated by elevating the pH of the solution to 7.8. The gelation process was examined using a time sweep at 1% strain and 1 Hz frequency. The strain range of 0.1%–1000% was covered by the strain amplitude sweep at a constant frequency of 1 Hz. All measurements were performed in triplicate at 37 °C.

2.3. 3D cell culture and cell viability

BMSCs, purchased from Procell Life Science & Technology Co., Ltd, were kept viable in growth medium (DMEM/F-12 with 10% FBS and 1% PS) at 37 °C and 5% CO_2. Every two days, the growth medium was changed, and the cells were passaged using 0.05% (w/v) trypsin with EDTA-4Na. The precursor solution was produced by dissolving HA-SH and PEG containing GSE4-SH in PBS. Later, BMSC pellets from passages 3–4 were disseminated at a cell density of 3 × 10^5 cells/mL to generate cell-laden hydrogels. The mixture was immediately transferred to a 24-well plate (Corning® Transwell®) after the pH was adjusted to 7.8. After gelation, growth medium was added on top of and surrounding the insert, and the cell-laden hydrogels were incubated at 37 °C with 5% CO_2. The media SAEpiCM was refreshed every 2 days. A DS-U3 digital camera on an Eclipse Ti-E microscope was used to capture images of the cells in hydrogels (Nikon, Tokyo, Japan). Live/dead staining was performed to measure the cell viability and cytotoxicity of BMSCs. The cell-laden HA/PEG/GSE4 hydrogels were thoroughly washed with PBS and then incubated in PBS containing Calcein-AM (4 mM) and PI (2 mM) for 15 min. A confocal laser scanning microscope (CLSM, FV3000, OLYMPUS, Japan) was used to observe the cells, and images were captured from three biological replicas as maximum intensity projections of approximately 200 μm thick z-stacks. Cell viability was measured as the ratio of live (green) cells to total cells.

2.4. Immunofluorescence

Cell-hydrogel samples were transferred to 8-well chambered cover glass after two weeks of growth. They were then incubated with Immunol Staining Fix Solution for 30 min, followed by three PBS washes. Each chambered cover glass was then covered with an Immunostaining Permeabilization Solution soaked for 45 min. After three washes with Immunol Staining Wash Buffer, each well was immersed for 1 h in Immunol Staining Blocking Buffer. The samples were then incubated in the primary antibody solution containing anti-Prosurfactant Protein C antibody produced by rabbits (or anti-Prosurfactant Protein B antibody produced by mouse) overnight at 4 °C. After a thorough wash with Immunol Staining Wash Buffer, the constructs were incubated for 2 h at room temperature in a secondary antibody solution containing Alexa Fluor® 594-conjugated goat anti-rabbit IgG (1:1000 dilution). Finally, the cell nuclei were stained for 10 min with DAPI solution.

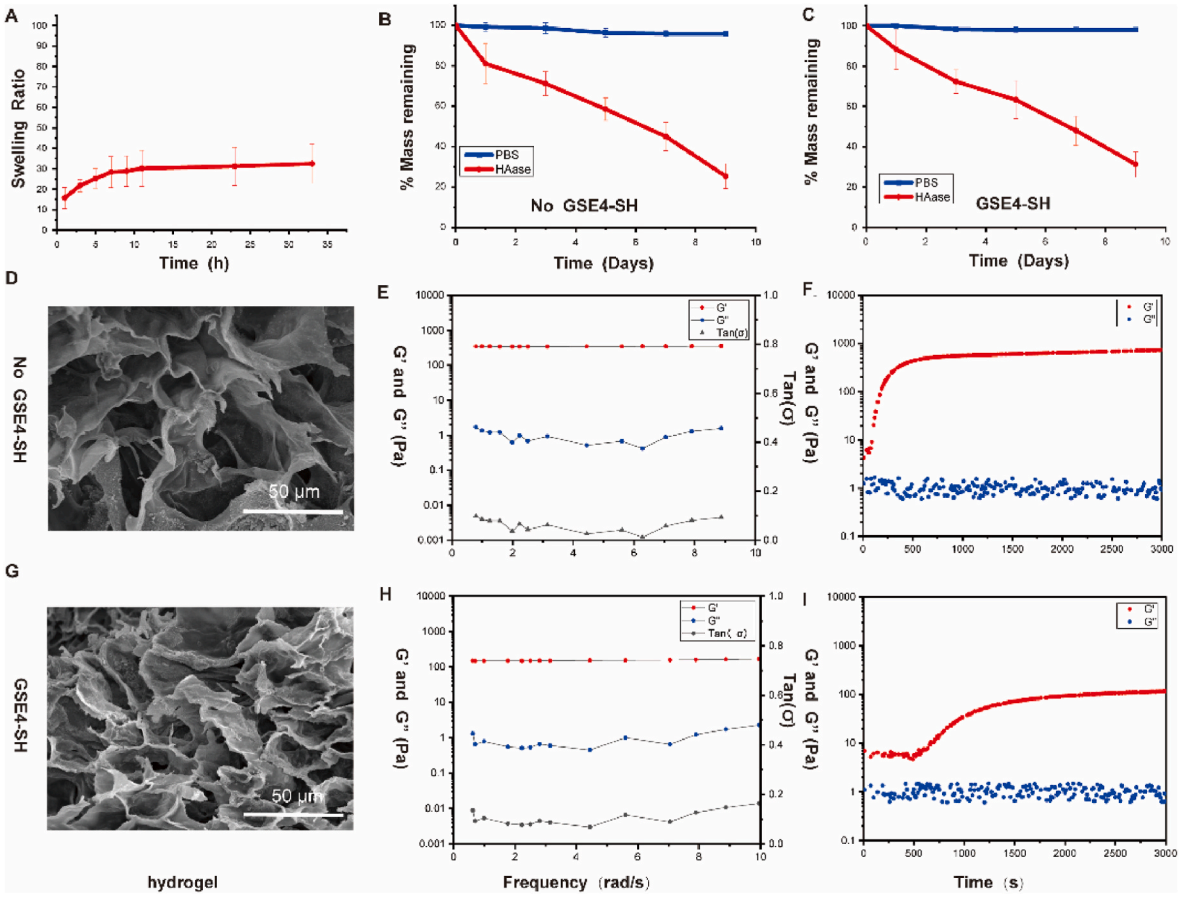

Fig. 3. Swelling kinetics of the hydrogel in PBS (A). Degradation of HA/PEG hydrogel (B) and HA/PEG/GSE4-SH (C) incubated in PBS 7.4 with or without 30 U/mL of HAase at 37 °C. SEM images of HA/PEG and HA/PEG/GSE4-SH hydrogels. Scale bar indicates 50 μm (D, G). Representative rheological frequency (E, H) and time sweep (F, I) measurements on HA/PEG and HA/PEG/GSE4-SH hydrogels.

Encapsulated cells were imaged by using a confocal laser scanning microscope (FV3000, OLYMPUS, Japan) with a maximum intensity projection of ~200 μm thick of z-stack after washing.

2.5. RT-qPCR

Total ribonucleic acid (RNA) was extracted from each hydrogel using TRIzol reagent (Invitrogen). Subsequently, using an ABI 7300 real-time PCR instrument, RT-qPCR experiment was carried out using SYBR green master mix, cDNA templates (4 ng), and primers (400 nM). Using commercially available qbase + software, data were normalized and processed with GAPDH as the reference target (Biogazelle, Zwijnaarde, Belgium). The primers are shown in Table S1 (Supplementary data). The data were calculated by using the $2^{-\Delta\Delta Ct}$ method. For each group, a total of three biological repeats were conducted, each with at least 5 different technical repeats. The mean and standard error of the mean (SEM) were utilized to represent the results.

2.6. Statistical analysis

One-way analysis of variance (ANOVA) was used for the comparisons across the data sets, and a p value of less than 0.05 was regarded as significant.

3. Results and discussion

3.1. Characterization and synthesis of hydrogel precursors

To obtain PEG/HA/GSE hydrogel, 4PEG-AC, HA-SH and GSE4-SH were designed as the core hydrogel precursors. 4PEG-AC has a long-term stable 4-arm acrylate groups [20], which are accessible to the cross-linking reaction with thiol groups. Thiolated hyaluronic acid (HA-SH) was synthesized as previously reported [21–23]. According to the ^{1}HNMR results in Fig. 2, HA was chemically modified with a latent disulfide molecule, followed by the cleavage of disulfide bond to yield HA-SH with an estimated thiolation of 23.5 mol%.

Dyskerin derived peptide GSE24.2 has been reported to enhance Telomerase Reverse Transcriptase (TERT) expression and protect cells from DNA damage [24,25]. GSE4 is a tiny fraction of GSE24.2 that consists of 11 amino acids and possesses the similar activity as GSE24.2. The amino acid sequence is GFINLDKPSNP. We here design a GSE peptide that retain its original biological function and possess enhanced water-solubility, as well as functional group for covalent bonding in hydrogel matrix. To this end, three glycine groups and one cysteine were added to the sequence to increase peptide solubility and to install a thiol group, respectively. As a result, a peptide with the sequence CGGGGFINLDKPSNP (abbreviated as GSE4-SH, a molecular weight of 1516.7 g/mol) was custom-synthesized and analyzed by high performance liquid chromatography and mass spectrometry.

3.2. Characterization and synthesis of hydrogel

PEG/HA/GSE4 and PEG/HA hydrogels were prepared by mixing 2 wt% HA-SH and 2 wt% 4PEG-AC with or without 2 mM GSE4-SH. Here, “click"-type chemical cross-linking was used for fast *in situ* hydrogel formation [14] by mixing HA-SH, GSE4-SH, and 4PEG-AC at pH 7.8, while the control group contained mixed HA-SH and PEG. The hydrogels exhibited a fast swelling in 2 h of immersion in PBS, reaching the

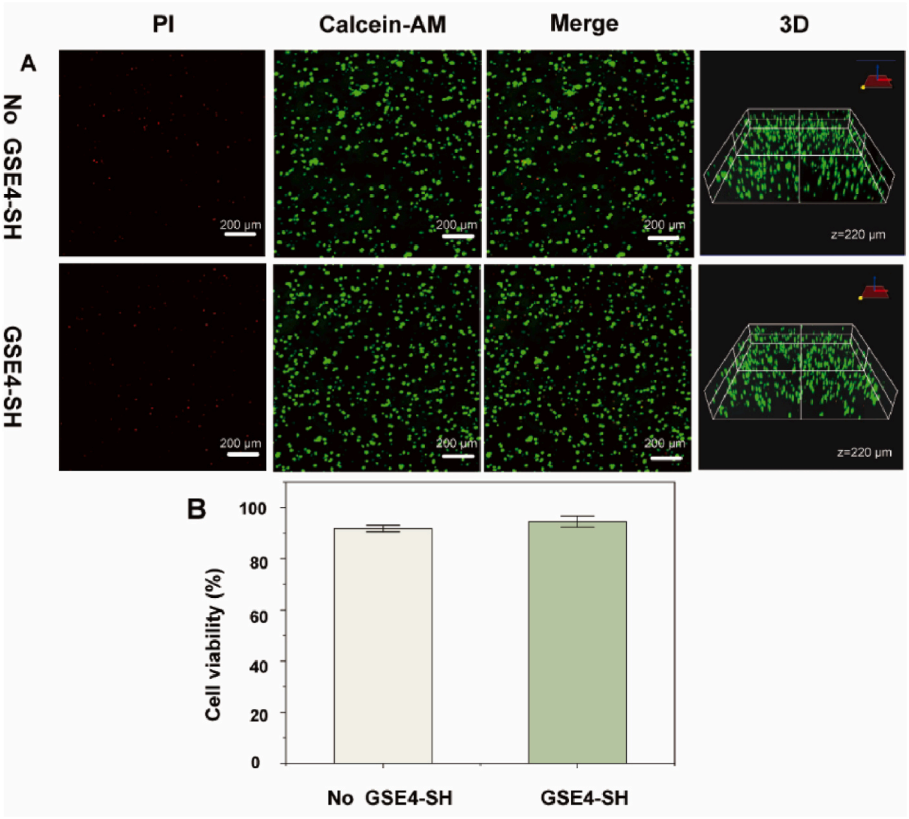

Fig. 4. (A) Representative confocal microscopy images and corresponding z-axis maximum projection image of live/dead stained BMSCs cultured in hydrogels at day 5. live (green) and dead (red) cells were stained by Calcein-AM and PI, respectively. Scale bar: 200 μm. (B) Quantification of cell viability based on live/dead assay using Image J. (For interpretation of the references to colour in this figure legend, the reader is referred to the Web version of this article.)

equilibrium swelling after 24 h according to Fig. 3A. As shown in Fig. 3B and C, for both condition, hydrogel can be degraded upon HAase treatment. It is noted that hydrogel degraded fast with ~25% mass remaining after 9 days in 30 U/mL HAase. The HAase concentration used in the degradation study was significantly higher than that in cell cultures or in tissues. Besides, hydrogel morphologies examined by SEM revealed the presence of interconnected pores in the matrix, as shown in Fig. 3D and G, indicating the 3D porous structures of hydrogel network.

In addition, the gelation kinetics and viscoelastic properties of the two groups of hybrid hydrogels were characterized by oscillatory rheology. The storage modulus (G′) and the loss modulus (G″) of the PEG/HA/GSE4 and PEG/HA hydrogels were measured using an oscillating time sweep and frequency sweep by rheometer. Fig. 3F and I show that gelation occurred rapidly once the pH of the two hydrogel precursor solutions approached to 7.8. Fig. 3F shows that the G′ value continued to increase, reaching a plateau modulus of 606 ± 70.8 Pa 15 min post-mixing. Fig. 3I reveals that G′ reached a plateau of 104.1 ± 9.9 Pa at 45 min. The PEG/HA/GSE4 group took longer to reach a plateau and had a lower G' value than that of HA/PEG group. The storage modulus was insensitive to frequency from 0 to 10 rad/S, and the two groups of corresponding tan(δ) (G″/G′) values were 0.006 ± 0.003 and 0.003 ± 0.001, respectively, demonstrating the elastic nature of the two groups of hydrogels.

In this work, G′ was noticeably reduced after the peptide was conjugated. Although previous study have demonstrated that the incorporation of 0.5 mM of matrix metalloproteinases peptide did not significantly affect the modulus of matrix [22]. The different observation can be ascribed to the increased concentration of GSE4-SH peptide (2 mM) and different peptide type. More peptide with –SH group consumed more acrylate groups, which might decrease the crosslinking density of the main network, leading to a decreased G′ value. Beside, Tan (δ) (G″/G′) was an indicator of the dynamic viscoelasticity of the polymer concentration. The smaller Tan(δ) reflected more elastic and solid-like systems. The tan(δ) values of the peptide group were smaller than those of the negative control group, indicating the predominance of the elastic component, which was consistent with the mechanical properties of the lung [26]. The lung's elastic network structure is formed by the ECM, which is primarily composed of elastin, collagen, and the surrounding matrix [27]. The energy storage modulus of the lung ECM is between 15 and 60 Pa, depending on the rheological characteristics of the lung [28]. Therefore, it can be inferred that the PEG/HA/GSE4 hydrogel could mimic ECM microenvironment of the lung and was suitable for the growth of lung cells.

3.3. Cell viability

PEG/HA/GSE4 and PEG/HA hydrogels were utilized for 3D culture of BMSCs, after 5 days of proliferation, the viability of BMSCs encapsulated in hydrogels were examined by using the calcein-AM/PI staining (calcein-AM, green; PI, red). The cytocompatibility of the hydrogels was also assessed. As shown in Fig. 4A, most of cells were live (green) with minimal cell death (red) and grow well in 3D matrix. According to the statistical results presented in Fig. 4B, the quantitative cell viabilities of the PEG/HA/GSE4 and PEG/HA groups were 94.5 ± 2.2% and 91.8 ± 1.2%, respectively, confirming the biocompatibility of both hydrogel systems for biomedical applications. Although not significant, GSE4 peptide group showed higher cell viability. The result validated the excellent biocompatibility of PEG and HA as the primary scaffold biomaterials [29–31].

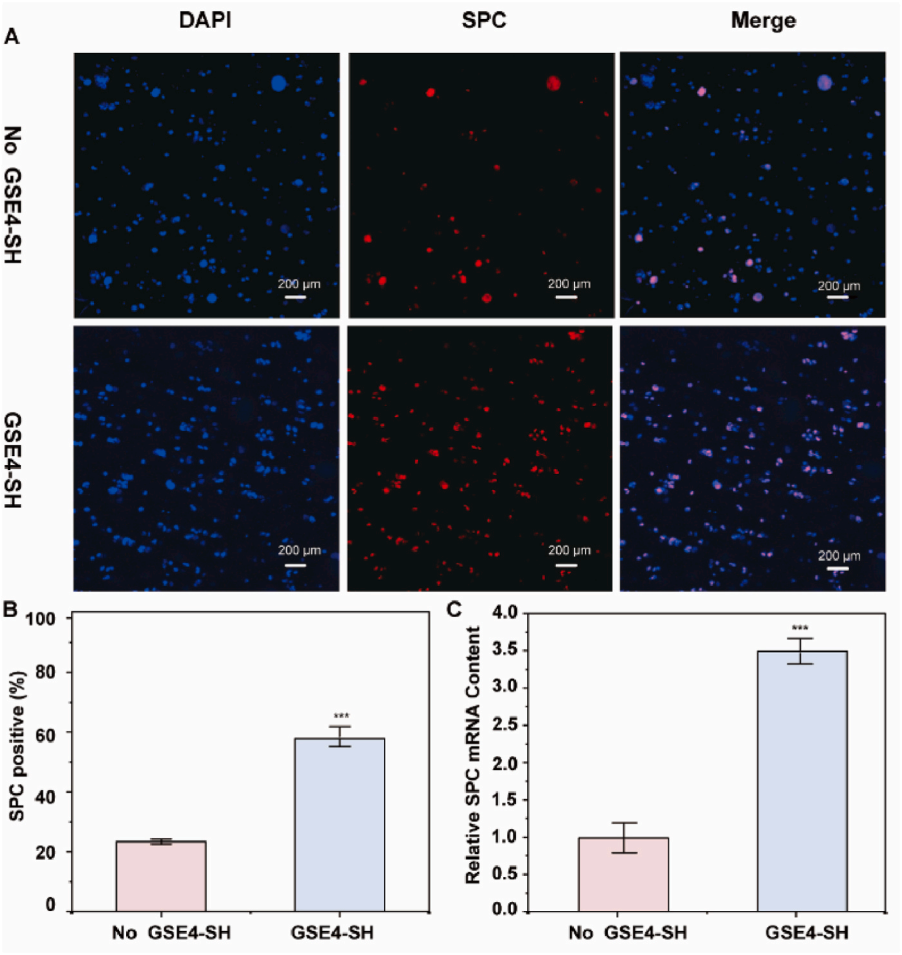

Fig. 5. (A) Representative confocal images of fluorescently stained BMSCs differentiation-cultured in hydrogels with or without GSE4-SH after 2 weeks. Cell nuclei and SPC were stained blue and red, respectively. Scale bar: 200 μm. (B) Quantification of SPC positive cells using Image J. (C) Quantification of gene expression by qPCR after 2 weeks of 3D culture. ***p < 0.001. (For interpretation of the references to colour in this figure legend, the reader is referred to the Web version of this article.)

3.4. Cell differentiation

BMSCs are excellent candidate cells for tissue engineering due to their capacity of multidirectional differentiation [32]. Hydrogels provide a 3D ECM-mimetic microenvironment for BMSCs growth and differentiation [18]. Next, BMSCs cultured in PEG/HA/GSE4 and PEG/HA hydrogels were induced to differentiate into lung cells AEC2s by suppling differentiation media SAEpiCM. Compared to the 2D culture showing spindle-like shape, most of cells encapsulated in the hydrogels exhibited round shape, while some are oblate spheroid (Figure S2, Supplementary data). Given that the overexpression of TERT promotes the differentiation of BMSCs [29], and GSE4 expression was found to stimulate the c-myc and TERT promoters, enhance the expression of TERT [18,30,31], BMSCs encapsulated in the PEG/HA hydrogel incorporated with GSE4-SH were expected to increase the expression levels of certain markers of AEC2s. To detect the SPC (a specific indicator for AEC2s [8,33,34]) expressions, immunostaining and qPCR were conducted. As shown in Fig. 5A, cells in both hydrogel systems expressed SPC, indicating the successful differentiation of BMSC into lung cells. Moreover, compared to the control group, BMSCs cultured in the PEG/HA/GSE4 hydrogel showed higher SPC expression, as confirmed by quantitative SPC-positive cell counting in Fig. 5B. The immunofluorescence-positive cell count was 58.57 ± 3.34% in the peptide group compared to 23.38 ± 0.84% in the non-peptide group. Similar enhancement can be observed for expression of another marker SPB [35], as shown in Figure S3 (Supplementary data), indicating that GSE4 facilitated the increased expression of AEC2s-relavant proteins. Additionally, according to the qPCR results in Fig. 5C, the relative SPC mRNA content was 3.49 ± 0.17 in the peptide group compared to 0.99 ± 0.2 in the non-GSE4 group. The mRNA expression levels of SPC were significantly increased in GSE4-present hydrogel, which was consistent with immunostaining results. GSE4-SH was chemically conjugated to the PEG/HA hydrogel scaffold. Thus, the covalent incorporation of peptide provided a stable stimulus for stem cell differentiation, thereby increasing the efficiency of AEC2s-differentiation.

4. Conclusions

In summary, a GSE4 peptide conjugated PEG/HA hydrogel was constructed from the crosslinking of acrylated 4-arm PEG, thiolated ECM-mimetic component HA, and thiolated GSE4 via Michael-type reaction. The generated PEG/HA/GSE4 hydrogel showed 3D porous network structure and viscoelastic properties, exhibiting excellent biocompatibility as a cell scaffold for BMSCs. PEG/HA/GSE4 hydrogel served as a supportive microenvironment for the cellular growth, as BMSCs encapsulated in hydrogel maintain high cell viability. Induced by SAEpiCM media, BMSCs cultured in PEG/HA/GSE4 hydrogel successfully differentiated into lung cells AEC2s. Notably, covalent incorporation of GSE4 peptide promoted the AEC2s-differentiation of BMSCs. These results demonstrate the great potentials of the engineering scaffold for lung tissue regeneration.

Funding

This work was supported by National Natural Science Foundation of China (51903246), Natural Science Foundation of Jiangsu Province (BK20201196), Suzhou Science and Technology Planning Project (SKY2021026) and Applied Medical Research Project of Hefei Municipal Health Commission (Hwk2021zd007).

Institution review board statement

Not applicable.

Informed consent statement

Not applicable.

CRediT authorship contribution statement

Xiaoqiong Wang: Investigation, Methodology, Software, Data curation, Writing – original draft. **Leisha Cui:** Visualization, Methodology. **Jing Hong:** Visualization, Methodology. **Zhaojun Wang:** Software, Validation. **Jiawei Li:** Methodology, Visualization. **Zhongqing Liu:** Methodology, Data curation. **Zhanchi Zhu:** Software, Data curation. **Ying Hao:** Conceptualization, Investigation, Writing – review & editing, Funding acquisition. **Guosheng Cheng:** Supervision, Investigation, Writing – review & editing. **Junhong Jiang:** Supervision, Investigation, Funding acquisition.

Declaration of competing interest

The authors declare that they have no known competing financial interests or personal relationships that could have appeared to influence the work reported in this paper.

Data availability

Data will be made available on request.

Abbreviations

BMSCs	Bone marrow mesenchymal stem cells
AEC1s	type I alveolar epithelial cells
AEC2s	type II alveolar epithelial cells
SAEpiCM	human small airway epithelial cells in complete medium
FDA	Food and Drug Administration
DTT	DL-Dithiothreitol
EDCI	N-(3-Dimethylaminopropyl)-N′-ethylcarbodiimide hydrochloride
DTP	3,3′-Dithiobis (propanoic dihydrazide)

Appendix A. Supplementary data

Supplementary data to this article can be found online at https://doi.org/10.1016/j.polymer.2023.125861.

References

[1] J.L. McQualter, D. Anthony, S. Bozinovski, C.M. Prele, G.J. Laurent, Int. J. Biochem. Cell Biol. 56 (2014) 82–91.
[2] R. Guillamat-Prats, G. Gay-Jordi, A. Xaubet, V.I. Peinado, A. Serrano-Mollar, J. Heart Lung Transplant. 33 (7) (2014) 758–765.
[3] R. Guillamat-Prats, M. Camprubi-Rimblas, F. Puig, R. Herrero, N. Tantinya, A. Serrano-Mollar, A. Artigas, Cells 9 (8) (2020) 1816.
[4] T. Zhang, J. Zhang, C. Lv, H. Li, X. Song, Front. Pharmacol. 13 (2022), 1059434.
[5] C.E. Barkauskas, M.J. Cronce, C.R. Rackley, E.J. Bowie, D.R. Keene, B.R. Stripp, S. H. Randell, P.W. Noble, B.L. Hogan, J. Clin. Invest. 123 (7) (2013) 3025–3036.
[6] L. Tamo, Y. Hibaoui, S. Kallol, M.P. Alves, C. Albrecht, K.E. Hostettler, A. Feki, J. S. Rougier, H. Abriel, L. Knudsen, A. Gazdhar, T. Geiser, Am. J. Physiol. Lung Cell Mol. Physiol. 315 (6) (2018) L921–L932.
[7] M. Zeng, Q. Chen, S. Ge, W. He, L. Zhang, H. Yi, S. Lin, Biochem. Biophys. Res. Commun. 528 (2) (2020) 311–317.
[8] N. Ma, H. Gai, J. Mei, F.B. Ding, C.R. Bao, D.M. Nguyen, H. Zhong, Cell Biol. Int. 35 (12) (2011) 1261–1266.
[9] A.R. Liu, L. Liu, S. Chen, Y. Yang, H.J. Zhao, L. Liu, F.M. Guo, X.M. Lu, H.B. Qiu, J. Cell. Physiol. 228 (6) (2013) 1270–1283.
[10] J. Liu, D. Peng, J. You, O. Zhou, H. Qiu, C. Hao, H. Chen, Z. Fu, L. Zou, Stem Cell. Dev. 30 (13) (2021) 660–670.
[11] E. Fukui, S. Funaki, K. Kimura, T. Momozane, A. Kimura, R. Chijimatsu, R. Kanzaki, T. Kanou, N. Ose, M. Minami, S. Miyagawa, Y. Sawa, M. Okumura, Y. Shintani, Stem Cell. Int. 2019 (2019), 5179172.
[12] F. Gao, J. Li, L. Wang, D. Zhang, J. Zhang, F. Guan, M. Yao, Biomed. Mater. 15 (4) (2020), 045013.
[13] D. Kouroupis, D. Correa, Front. Bioeng. Biotechnol. 9 (2021), 621748.
[14] Z. Liu, M. Tang, J. Zhao, R. Chai, J. Kang, Adv. Mater. 30 (17) (2018), e1705388.
[15] J. Nicolas, S. Magli, L. Rabbachin, S. Sampaolesi, F. Nicotra, L. Russo, Biomacromolecules 21 (6) (2020) 1968–1994.
[16] S. Ma, B. Yu, X. Pei, F. Zhou, Polymer 98 (2016) 516–535.
[17] C.-G. Miryam, R. Jean-Yves, C. Alain, B. Fouzia, W. Pierre, S. Pierre, J. Loïc, Polymer (2022), 125398.
[18] X. Hu, Z. Xia, K. Cai, J. Mater. Chem. B (2022) 486–507.
[19] L.A. Gurski, X. Xu, L.N. Labrada, N.T. Nguyen, L. Xiao, K.L. van Golen, X. Jia, M. C. Farach-Carson, PLoS One 7 (11) (2012), e50075.
[20] M.D. Hunckler, J.D. Medina, M.M. Coronel, J.D. Weaver, C.L. Stabler, A.J. Garcia, Adv. Healthc. Mater. 8 (14) (2019), e1900371.
[21] Y. Hao, A.B. Zerdoum, A.J. Stuffer, A.K. Rajasekaran, X. Jia, Biomacromolecules 17 (11) (2016) 3750–3760.
[22] Y. Hao, J. Song, A. Ravikrishnan, K.T. Dicker, E.W. Fowler, A.B. Zerdoum, Y. Li, H. Zhang, A.K. Rajasekaran, J.M. Fox, X. Jia, ACS Appl. Mater. Interfaces 10 (31) (2018) 26016–26027.
[23] Y. Hao, J. He, X. Ma, L. Feng, M. Zhu, Y. Zhai, Y. Liu, P. Ni, G. Cheng, Carbohydr. Polym. 225 (2019), 115257.
[24] L. Iarriccio, C. Manguan-Garcia, L. Pintado-Berninches, J.M. Mancheno, A. Molina, R. Perona, L. Sastre, GSE4, PLoS One 10 (11) (2015), e0142980.
[25] L. Pintado-Berninches, B. Fernandez-Varas, C. Benitez-Buelga, C. Manguan-Garcia, A. Serrano-Benitez, L. Iarriccio, J. Carrillo, G. Guenechea, S.P. Egusquiaguirre, J. L. Pedraz, R.M. Hernandez, M. Igartua, E.G. Arias-Salgado, F. Cortes-Ledesma, L. Sastre, R. Perona, Cell Death Differ. 26 (10) (2019) 1998–2014.
[26] H.M. Beni, H. Mortazavi, M.S. Islam, Biomech. Model. Mechanobiol. 21 (1) (2022) 79–87.
[27] J.C. Valdoz, N.A. Franks, C.G. Cribbs, D.J. Jacobs, E.L. Dodson, C.J. Knight, P. D. Poulson, S.R. Garfield, B.C. Johnson, B.M. Hemeyer, M.T. Sudo, J.A. Saunooke, B.C. Kartchner, A. Saxton, M.L. Vallecillo-Zuniga, M. Santos, B. Chamberlain, K. A. Christensen, G.P. Nordin, A.S. Narayanan, G. Raghu, P.M. Van Ry, Biomaterials 283 (2022), 121464.
[28] R.A. Pouliot, P.A. Link, N.S. Mikhaiel, M.B. Schneck, M.S. Valentine, F.J. Kamga Gninzeko, J.A. Herbert, M. Sakagami, R.L. Heise, J. Biomed. Mater. Res. 104 (8) (2016) 1922–1935.
[29] C. Qu, Z. Bao, X. Zhang, Z. Wang, J. Ren, Z. Zhou, M. Tian, X. Cheng, X. Chen, C. Feng, Int. J. Biol. Macromol. 125 (2019) 78–86.
[30] X. Li, Y. Teng, J. Liu, H. Lin, Y. Fan, X. Zhang, J. Mater. Chem. B 5 (26) (2017) 5109–5119.
[31] C. Liu, Q. Yu, Z. Yuan, Q. Guo, X. Liao, F. Han, T. Feng, G. Liu, R. Zhao, Z. Zhu, H. Mao, C. Zhu, B. Li, Bioact. Mater. (2022) 31, https://doi.org/10.1016/j.bioactmat.2022.07.031.
[32] G. Bi, S. Liu, X. Zhong, Y. Peng, W. Song, J. Yang, L. Ren, Macromol. Biosci. (2022), e2200250.
[33] Y. Xi, T. Kim, A.N. Brumwell, I.H. Driver, Y. Wei, V. Tan, J.R. Jackson, J. Xu, D. K. Lee, J.E. Gotts, M.A. Matthay, J.M. Shannon, H.A. Chapman, A.E. Vaughan, Nat. Cell Biol. 19 (8) (2017) 904–914.
[34] X. Jing, W. Sun, X. Yang, H. Huang, P. Wang, Q. Luo, S. Xia, C. Fang, Q. Zhang, J. Guo, Z. Xu, Int. J. Biochem. Cell Biol. 143 (2022), 106142.
[35] T. Wu, S.A. Rabi, W.A. Michaud, D. Becerra, S.E. Gilpin, M. Mino-Kenudson, H. C. Ott, Biomaterials 285 (2022), 121509.